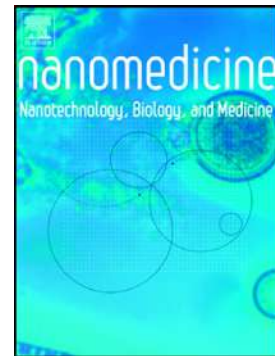


Accepted Manuscript

Raman spectral signatures of urinary extracellular vesicles from diabetic patients and hyperglycemic endothelial cells as potential biomarkers in diabetes

Maciej Roman, Agnieszka Kamińska, Anna Drożdż, Mark Platt, Marek Kuźniewski, Maciej T. Małecki, Wojciech Kwiatek, Czesława Paluszkiewicz, Ewa Ł. Stępień



PII: S1549-9634(19)30023-1

DOI: <https://doi.org/10.1016/j.nano.2019.01.011>

Reference: NANO 1943

To appear in: *Nanomedicine: Nanotechnology, Biology, and Medicine*

Revised date: 18 December 2018

Please cite this article as: M. Roman, A. Kamińska, A. Drożdż, et al., Raman spectral signatures of urinary extracellular vesicles from diabetic patients and hyperglycemic endothelial cells as potential biomarkers in diabetes, *Nanomedicine: Nanotechnology, Biology, and Medicine*, <https://doi.org/10.1016/j.nano.2019.01.011>

This is a PDF file of an unedited manuscript that has been accepted for publication. As a service to our customers we are providing this early version of the manuscript. The manuscript will undergo copyediting, typesetting, and review of the resulting proof before it is published in its final form. Please note that during the production process errors may be discovered which could affect the content, and all legal disclaimers that apply to the journal pertain.

Raman spectral signatures of urinary extracellular vesicles from diabetic patients and hyperglycemic endothelial cells as potential biomarkers in diabetes

Maciej Roman^{a,*}, Agnieszka Kamińska^{b,*}, Anna Drożdż^b, Mark Platt^c, Marek Kuźniewski^d,

Maciej T. Malecki^e, Wojciech Kwiatek^a, Czesława Paluszkiewicz^a, Ewa Ł. Stepien^b

^aInstitute of Nuclear Physics, Polish Academy of Sciences, Krakow, 31-342, Poland, e-mail: maciej.roman@ifj.edu.pl, czeslawa.paluszkiewicz@ifj.edu.pl, wojciech.kwiatek@ifj.edu.pl

^bDepartment of Medical Physics, Marian Smoluchowski Institute of Physics, Faculty of Physics, Astronomy and Applied Computer Science, Jagiellonian University, Krakow, 30-348, Poland, e-mail: agnieszka1.kaminska@uj.edu.pl, anna.drozd@uj.edu.pl, e.stepien@uj.edu.pl

^cDepartment of Chemistry, Loughborough University, Loughborough, LE11 3TU, United Kingdom, e-mail: m.platt@lboro.ac.uk

^dDepartment of Nephrology, Jagiellonian University Medical College, Krakow, 31-501, Poland, e-mail: marek.kuzniewski@uj.edu.pl

^eDepartment of Metabolic Diseases, Jagiellonian University Medical College, Krakow, 31-501, Poland, e-mail: maciej.malecki@uj.edu.pl

**Corresponding authors*

Agnieszka Kamińska
Department of Medical Physics
Marian Smoluchowski Institute of Physics,
Faculty of Physics, Astronomy and Applied Computer Science
Jagiellonian University
Łojasiewicza 11 Street, 30-348 Kraków, Poland
Tel: +48 785 777 921, Fax: 12 664 49 05

Word count for abstract: 150
Complete manuscript word count: 4836
Number of figures: 8
Number of tables: 1
Number of references: 49

Grants:

The project co-funded by the Małopolska Regional Operational Program Measure 5.1 Krakow Metropolitan Area as an important hub of the European Research Area for 2007- 2013, project No. MRPO.05.01.00-12-013/15 and Polish National Centre (NCN) the grant OPUS 4 (2012/07B/NZ5/02510).

Conflict of Interest: There are no conflicts to declare.

Abstract

Raman spectroscopy was applied to the measurement of urinary and *in vitro* endothelium-derived extracellular vesicles (EVs) isolated by hydrostatic filtration dialysis (HFD) method. Raman spectra obtained for urinary EVs (UEVs) showed distinct differences in the fingerprint region. In contrast, average Raman spectra of endothelium-derived EVs samples were almost identical. Cluster Analysis of UEVs significantly discriminated diabetic samples from control, moreover endothelium-derived EVs revealed stronger similarity between long hyperglycemia and normoglycemia samples compared to short hyperglycemia. Results obtained from Partial Least Squares analysis corresponded well with integral intensities of selected bands.

Our proof-of-concept approach demonstrates the potential for Raman spectroscopy to be used both for identification of EVs molecular signatures in urine samples from patients with type 2 diabetes mellitus and good glycemic control and unsatisfactory glycemic control as well as for *in vitro* hyperglycemic model. This non-invasive technique may be useful in identifying new biomarkers of diabetes and renal complications.

Keywords

diabetes mellitus, extracellular vesicles, partial least squares regression, Raman spectroscopy signature, urine

1. Background

The last decade has seen an increase in research within the field of cell-derived extracellular vesicles (EVs). These nano-sized membranous vesicles play a crucial role in many biological processes such as: coagulation and fibrinolysis, intercellular communication, inflammation and angiogenesis [1-4]. Due to their presence in almost all body fluids, EVs appear as potential biomarkers of diseases [5, 6]. Urine has shown to be a particularly rich reservoir of EVs released by glomerular epithelial cells which line the urinary tract [6]. The number of EVs in urine has been shown to correlate with endothelium function in diabetic nephropathy [7]. This makes urine of great interest for diagnostic application because of easy and non-invasive collection way. Urinary EVs (UEVs) contain different biomolecules such as proteins, nucleic acids (DNA, mRNAs, microRNAs, small RNAs) and lipids [5]. Both major forms of diabetes, type 1 (T1DM) and type 2 diabetes mellitus (T2DM) are frequently complicated by different stages of diabetic nephropathy. Endothelial dysfunction and podocyte loss are key elements of its pathogenesis. It has been suggested that number and content of UEVs can reflect the stage of renal damage in diabetes [7-9].

Endothelium-derived EVs can be isolated from cell culture medium as an *in vitro* model of endothelial dysfunction [10]. EVs are formed by endothelial cells upon activation, apoptosis or other processes leading to endothelial dysfunction like: tumor necrosis factor-alpha (TNF- α), oxidative stress, increased homocysteine levels or hyperglycemic state [10, 11]. Proteomic analyses showed that endothelium-derived EVs contain a huge number of specific proteins which can be transferred over long distances and interact with target cells [12].

Many optical and non-optical techniques have been used for several decades to characterize EVs, including high-resolution imaging with electron microscopy, nanoparticle tracking analysis (NTA), dynamic light scattering (DLS), tunable resistive pulse sensing (tRPS), flow

cytometry, atomic force microscopy and many others [13-15]. To date, none of these techniques have proven to be without limitations and the EV community have not adopted a “gold standard” protocol for analysis. A technology gap exists for any method that can explore physical and chemical characteristics of EVs. Raman spectroscopy is a non-destructive, label-free method, based on inelastic scattering of monochromatic light which provides information about chemical content of EVs [16-18]. Raman spectroscopy has found applications within varied fields of science that include pharmacy, cosmetology, geology and carbon material or life sciences. This technique can also be used in forensic medicine to identify bloodstain evidences based on Raman spectrum of a single red blood cell [19-21]. Furthermore, Raman spectroscopy is a promising tool for clinical applications because it enables specific detection of hemoglobin and albumin glycation which can be useful for diabetes monitoring [22-24]. Urine, which contains a large number of different metabolites and waste products, has a very large diagnostic potential. For example, the spectral signature obtained by Raman spectroscopy of urine samples of healthy and cancer patients may discriminate healthy subjects from affected individuals even in the early stage of disease [25].

Taking into account the potential usefulness of circulating and UEVs as biomarkers of diseases, we explored the application of Raman spectroscopy in laboratory medicine to distinguish T2DM patients and healthy controls based on the Raman spectra characteristic. Additionally, we used the spectral signature to compare diabetic patients having a glycemic control on different levels.

To reveal the role of hyperglycemia in endothelial cell function, we analysed the Raman spectra of EVs isolated from our *in vitro* hyperglycemia model – human umbilical cord endothelial cell (HUVEC) culture, as the pilot experiment.

2. Methods

Study groups

Forty five T2DM patients (14 women and 31 men) were enrolled to the present study. Patients were divided into two groups: CD – individuals with good glycemic control (n=19) and UD – subjects with unsatisfactory glycemic control (n=26). Patients with the HbA1c level above 7% were considered to have unsatisfactory glycemic control, as recommended by guidelines in diabetes care [26]. Additionally, 10 healthy subjects (5 women and 5 men) were included to the study. Information about blood samples collection, measurement of biochemical parameters and differences between study groups are described in Supplementary Methods.

Urine samples collection and isolation of UEVs

UEVs were isolated accordingly to Musante et al. [27] with some modifications. Briefly, first morning urine specimens were collected in a sterile container from diabetic patients and healthy subjects. Urine was tested with Urisys 2400 analyzer (Roche Diagnostics, IN, USA). Urine samples (5 mL from each person) were pooled together in each study group (CD, UD and control) and centrifuged in a Hermle Z300K for 30 min in 2000 x g at room temperature (RT) to remove cell debris, polymers of Tamm-Horsfall protein and majority of urinary bacteria. Directly after centrifuge stops supernatants were collected. Before freezing in -80°C, sodium citrate and EDTA were added to supernatant (final concentration 50 mM and 8 mM, respectively) to prevent calcium oxalate crystals formation. Before further procedure of UEVs purification, frozen samples were thawed in 37°C and colloidal silver solution (0.1 mg silver chloride and 4.5 mg troclosen sodium per 1 litre of urine) was added. Hydrostatic Filtration Dialysis (HFD) of pooled supernatants from each group was performed using dialysis cellulose membrane with molecular weight cut-off (MWCO) 1,000 kDa. After sample

concentration to 3 mL, membrane was refilled with 100 mL of demineralized water and filtration was kept until the volume of around 1 mL was reached. The retained solution was ultracentrifuged for 1.5 hour in 100 000 x g at 4°C (Optima™ MAX-XP, Beckman Coulter Life Sciences, Indianapolis, USA) using fixed angle rotor (MLA-130, Beckman Coulter Life Sciences, Indianapolis, USA). Obtained UEVs pellet was suspended in demineralized water or in PBS and used for Raman Spectroscopy analysis and tRPS analysis, respectively. Schematic procedure of UEV isolation is presented in Supplementary Fig. S1, A.

Hyperglycemia cell culture and isolation of endothelium-derived EVs

Human Umbilical Vein Endothelial Cells (HUVECs) were isolated from umbilical cord resected immediately after childbirth. HUVECs were grown in a cell culture media consisting of a serum-free media-SFM (45%) and 199 media (45%), supplemented with 10% FBS and penicillin/streptomycin antibiotics at 37°C and 5% CO₂. Part of the cells were cultured under normoglycemic conditions (5 mM), while another cells were cultured under short (1 passage) and long-term (3 passages) hyperglycemic conditions (25 mM). Endothelium-derived EVs were isolated from culture media after 24h serum starving conditions. After cells reached minimum 90% of confluence, 30 mL of cell culture conditioned media were collected. Immediately after collection, media were centrifuged in an Eppendorf 5810/5810R centrifuge (Eppendorf AG, Hamburg, Germany) for 30 min in 2000 x g (at the top of the tube) at RT to remove cell debris. The HFD method was used for further endothelium-derived EVs purification as was described in the previous paragraph. Schematic procedure of UEV isolation is presented in Supplementary Fig. S1, B.

Raman Spectroscopy

Raman spectra were recorded using a Renishaw InVia Raman spectrometer equipped with an optical confocal microscope, an air-cooled laser emitting at 532 nm, and a CCD detector

thermoelectrically cooled to -70°C . The dry Leica N PLAN EPI (100x, NA 0.85) objective was used. The power of the laser at the sample position was ca. 15 mW. A drop of UEVs suspension (of each sample) was spotted onto a CaF_2 window and left for water evaporation. Each dried sample (six samples in total: C, CD, UD, NG, HG long, HG short) was measured in at least 15 places. A sum of 100 scans with integration time of 20 s and a resolution of 1.5 cm^{-1} was collected from each place. The spectrometer was calibrated using the Raman scattering line generated by an internal silicon plate. Cluster Analysis (CA) was performed using the OPUS 7.5 software (Bruker, Germany) and Partial Least Squares (PLS) regression was carried out using the MatLab R2017b software (MathWorks, Inc., USA). Prior to analysis, Raman spectra were baseline corrected, smoothed, and normalized. When necessary, cosmic ray removal procedure was applied. Supplementary Fig. S1, C shows schematic summary of EV measurement by Raman Spectroscopy technique.

Ethical consideration

This study was approved by The Bioethical Committee of Jagiellonian University in Krakow which accepted all project's protocols and forms, including an information for patients form and a consent form. The permission No. KBET/206/B/2013 was extended until 31st December 2017 and the permission No. 122.6120.78.2016 valid until 30th April 2018.

Statistical analysis

The data analysis was performed using the Statistica 12 (Dell Statistica, Tulsa, USA) and OriginPro 2016 (OriginLab Co., Northampton, MA, USA). The distribution of continuous data was verified with Shapiro-Wilk normality test. Results are expressed as mean (SD) for data with normal distribution or median and interquartile ranges (Q1-Q3) for data with not normal distribution. The one-way analysis of variance ANOVA or Kruskal-Wallis test were used for comparison of biochemical parameters among control and diabetic patients groups.

Differences between subgroups were tested with t-Student or Mann-Whitney U test. For integral intensity analysis one-way ANOVA followed by Bonferroni correction test was employed. For all analyses p-value<0.05 were considered to be significant.

3. Results

Study groups characteristics – urine and blood biochemistry and EV concentration

Clinical characteristics of the study groups are shown in Table 1. Patients with good (CD) and unsatisfactory glycemic control (UD) had significantly higher level of serum glucose (6.8 vs. 5.2 mmol/L; $p<0.0001$) and (8.8 vs. 5.2 mmol/L; $p<0.0001$) and lower urine creatinine concentration (5.4 vs. 12.2 mmol/L; $p=0.01$) and (6.3 vs. 12.2 mmol/L; $p=0.005$) with comparison to the control group. The UD patients had significantly higher level of serum glucose than CD group (8.8 vs. 6.8 mmol/L, $p=0.004$). There was a significant difference in HbA1c level between CD and UD patients (44 vs. 68 mmol/mol; $p<0.0001$). The UD patients had significantly higher albumin level with comparison to CD and control group (29.9 vs. 6 mg/L; $p=0.0002$) and (29.9 vs 6.2 mg/L; $p=0.008$), respectively. There was not a statistically significant difference in the average EVs concentration between study groups, but we found difference in median size diameter between C and UD group (121 vs. 128 nm; $p=0.005$) and C and CD group (121 vs. 135 nm; $p=0.0002$).

Raman Spectroscopy analysis of UEVs

Average Raman spectra of samples from the study groups are presented in Figure 1, A. It can be seen that all three spectra show distinct differences in the fingerprint region. For instance, Raman spectra of the CD and UD samples exhibit higher relative intensities of bands in the region of 600 – 950 cm^{-1} when compared to the control group (healthy subjects). Control and diabetic samples differ also in relative intensities of the Amide I (1670 cm^{-1}) band. However, detailed analysis of all chemical differences between the samples requires application of more

advanced chemometric methods such as Cluster Analysis (CA) and Partial Least Squares regression (PLS regression). All collected spectra were firstly tested for their heterogeneity using CA method. The results are shown in Figure 1, B. As can be seen, diabetic samples show much higher similarity between each other when compared to the control ones. Moreover, CA method allows also distinguishing between CD and UD samples, with some limitations due to much stronger similarity between these two groups, which makes some spectra grouped incorrectly.

In the second step of the analysis, PLS method was applied to study spectral differences between the investigated samples. In the first approach, a model for all three samples was built to find correlation between chemical changes and type of disease (diabetic patients with good and unsatisfactory glycemic control). However, as it was already mentioned, CA results shows stronger similarity between CD and UD samples when compared to the control. Thus, assigned variables (1 for control, 0 for CD, -1 for UD) were optimized to find the highest value of explained variance by the first Latent Variable (LV) (Supplementary Table S1). The highest variance was found for two sets of variables, *i.e.* -0.85 for control, -1 for CD, and 1 for UD as well as 1 for control, -1 for CD, and -0.25 for UD. The first set of variables has higher value of explained variance (77.25%) when compared to the second one (69.10%). However, the second set of variables confirms observations from CA analysis (Figure 1, B). Both sets of variables were applied for PLS analysis and the results are gathered in Figure 2. As can be seen in Figure 2, A, only two groups of samples can be easily distinguished using the CD-C-UD model, *i.e.* C-CD group and UD samples. The regression coefficient plot (Figure 2, C) indicates several bands to be responsible for separation between the studied groups. The most distinct difference is observed for proteins, lipids, and DNA/RNA bands. The control and CD samples show much higher relative intensities of β -sheet protein bands when compared to the UD ones. It can be observed as negative peaks with maxima at 1062,

1127, 1232, and 1684 cm^{-1} [31-33]. On the other hand, Raman spectra of UD samples show higher relative intensities of phenylalanine bands observed as positive bands with maxima at 1002 and 1600 cm^{-1} [31-33]. It suggests lower total content of proteins in the UEVs of UD patients, but higher content of some phenylalanine-rich protein groups. Additionally, UD samples exhibit higher lipid content. Lipid bands can be found at 539, 959, 1085, 1307, 1437, and 1470 cm^{-1} [31, 32, 34]. On the other hand, control and CD samples show higher content of nucleic acids (DNA/RNA), what can be observed as negative signals located at 669, 789, 815, 1103, and 1232 cm^{-1} [31, 32]. Moreover, UD samples show a distinct band at 853 cm^{-1} , which can be assigned to 3-hydroxybutyric acid (HA) [35] – a main component of ketone bodies [36]. All three samples (C,CD,UD) can be distinguished using the CD-UD-C model (Figure 2, D). The regression coefficient plot (Figure 2, F) indicates spectral pattern responsible for separation between the studied groups. The most distinct difference is observed for proteins, lipids, and nucleic acids (DNA/RNA) bands. Main positive bands can be observed at 445, 700, 719, 852, 880, 956, 1006, 1087, 1436, 1471, and 1669 cm^{-1} . It suggests higher content of proteins in random coil conformation and lipids (cholesterol and choline) in control and UD samples [31-34]. On the other hand, distinct negative bands can be found at 584, 668, 789, 815, 1231, 1295, and 1395 cm^{-1} . Most of the bands can be assigned to nucleic acids [31,32], what suggests higher content of these biomolecules in CD samples.

It is vitally important to notice that the content of UEVs for healthy subjects and T2DM patients with good and unsatisfactory glycemic control can be chemically different. Thus, it seems necessary to find detailed spectral differences between all types of the samples.

PLS (regression coefficient) plots for C-CD, C-UD, and CD-UD sample pairs are shown in Figure 3. Control samples show higher relative intensity of some lipids (mainly cholesterol and choline) as well as β -sheet proteins (Amide I band) (Figure 3, A). On the other hand, CD samples exhibit higher content of DNA/RNA (750 – 850 cm^{-1} region). The C-UD plot (Figure

3, B) shows similar pattern, however; some distinct differences in some spectral regions can be easily noticed. These discrepancies are related to the differences between Raman spectra of control and CD samples. As can be seen, regression coefficient plots for C-CD, C-UD sample pairs (Figures 3, A and 3, B) exhibit similar pattern as regression coefficient plots for the CD-UD-C model (Figure 2, F). On the other hand, the CD-UD plot is exactly the same as the regression coefficient plot obtained from the CD-C-UD model (compare Figure 3, C with Figure 2, C).

Additionally, results obtained from PLS analysis were compared with calculation of integral intensities of selected bands (see Supplementary Fig. S2 and Supplementary 1).

Finally, it is of great interest to compare spectral data with clinical characteristics (blood and urine biochemistry, Table 1). Figure 4 shows comparison of predicted and measured clinical parameters as well as regression coefficient β plots calculated from PLS models for correlations between Raman spectra of CD, C, UD samples and three blood/urine compounds, which show statistically significant differences in concentrations between the individual sample groups (see Table 1). As can be seen from Figure 4, A, measured Raman spectra correlate well with serum glucose concentration, however; the first LV explains only *ca.* 38% of variance (Supplementary Table S2). Additionally, serum glucose concentration is significantly higher for CD samples when compared to the control ones, whereas the CD-C-UD model (Figure 2, A-C) did not show separation between these samples. Nevertheless, PLS method can be used to characterize spectral changes in Raman spectra, which correlate with serum glucose concentration. As can be seen, regression coefficient β plot for serum glucose model (Figure 4, B) exhibits almost the same spectral pattern as the CD-C-UD plot (Figure 2, C). It shows positive bands mainly for phenylalanine (1000 and 1600 cm^{-1}) and HA (474 and 853 cm^{-1}) as well as negative bands for proteins in β -sheet conformation (444 , 508 , 1063 ,

1128, 1234, 1639, 1681 cm^{-1}) [31-33, 37]. Similar correlation can be obtained for urine albumin (Figure 4, C). It is worth noting that C and CD samples exhibit almost the same albumin concentration in urine (Table 1). Thus, it is obvious that PLS model for urine albumin is very similar to the CD-C-UD model (Figure 2, A-C). Indeed, inspection of Figure 4, D points to the conclusion that spectral changes found by this model are exactly the same as obtained from the CD-C-UD model (Figure 2, C) and similar to those obtained from PLS model for serum glucose (compare Figure 4, D with Figure 4, B). As can be seen, urine albumin PLS model shows very strong similarity between C and CD samples and high heterogeneity of UD samples, which is in accordance with the results obtained from the CD-C-UD model. On the other hand, Figure 4E shows correlation between Raman data and urine creatinine concentration, which assumes much stronger similarity between CD and UD samples as it was observed in CA analysis. Indeed, model obtained from PLS method allows clear separation between C and CD/UD samples, whereas separation between CD and UD samples is not complete. As can be seen from Figure 4F, spectral changes are almost the same as calculated for the CD-UD-C model (Figure 2, F).

Raman Spectroscopy analysis of endothelium-derived EVs

Average Raman spectra of control (normoglycemic, NG) and hyperglycemic (HG long and HG short) endothelium-derived EVs are shown in Figure 5, A. As can be seen, the spectra are almost identical showing slight differences in intensities of some bands. Similarly, to the previous case, analysis of the samples was performed with the support of CA and PLS methods. The level of heterogeneity of Raman spectra is shown as the CA results obtained for all endothelium-derived EV groups (Figure 5, B). As can be seen, the groups can be successfully separated using three clusters, however; HG long samples seem to be more similar to controls (NG) rather than to HG short ones.

In the next step, PLS method was applied as it was performed for samples of diabetic patients. Since CA analysis shows stronger similarity between HG long and NG samples, assigned variables (-1 for NG, 0 for HG long, 1 for HG short) were also optimized to find the highest value of explained variance by the first LV (Supplementary Table S3). Only one distinct maximum was found with the following variable values: -1 for NG, -0.75 for HG long, and 1 for HG short. Results of PLS analysis for such a set of variables is presented in Figure 6. As can be seen in Figure 6, A, all three sample groups can be distinguished using the obtained model. The regression coefficient plot (Figure 6, C) indicates several bands to be responsible for separation between the studied groups. Positive bands (HG short samples) can be assigned to saccharides (543, 838, 919, 1354 cm^{-1}), proteins in random coil conformation (1002, 1152, 1171, 1230, 1551, 1568, 1582, 1669 cm^{-1}) as well as lipids and phospholipids including cholesterol and its derivatives (421, 698, 716, 875, 983, 1130, 1397, 1435, 1703 cm^{-1}) [30-33]. On the other hand, negative bands (NG and HG long) are characteristic for DNA/RNA and amino acids (664, 784, 1102, 1189, 1291 cm^{-1}) and proteins in α -helix conformation (639, 907, 937, 1062, 1335, 1649 cm^{-1}) [31-33].

As it was mentioned previously, it is important to find spectral differences between individual sample groups as well. Figure 7, A shows regression coefficient β plot calculated for NG – HG short sample pair. It is obvious that this plot looks almost the same as regression coefficient β plot for all groups (Figure 6, C), however, it is much less noisy. Similar spectral pattern can be observed for HG long – HG short plot (Figure 7, B). Apart from some slight differences in band intensities, especially in the region of 1100 – 1200 cm^{-1} , both plots exhibit exactly the same bands to be responsible for differentiation between HG short and NG/HG long samples. Thus, PLS analysis confirms strong similarity between control (NG) and HG long samples. However, it is also possible to distinguish NG and HG long samples. Figure 7, C shows regression coefficient β plot calculated for these two groups of samples. As can be

seen, the plot is very noisy, but some distinct bands can be easily observed. Indeed, HG long samples exhibit much higher content of saccharides (main band at 540 cm^{-1}) and RNA (characteristic band at 816 cm^{-1}). Additionally, some protein bands can be observed as positive signals, especially coming from phenylalanine and tryptophan vibrations (1004 , 1207 , 1360 , 1586 , 1604 cm^{-1}). On the other hand, control samples show other protein bands (*e.g.* 615 , 639 , 761 , 934 , 1021 , 1235 , 1544 cm^{-1} and the Amide I bands) [33].

Results obtained from PLS were also compared with calculation of integral intensities of selected bands (see Supplementary Fig. S3 and Supplementary 2).

TEM images of UEVs and endothelium-derived EVs in normoglycemic and hyperglycemic conditions

Representative optical microscopy images of HUVEC cells cultured in normoglycemic and hyperglycemic conditions do not show any changes in endothelial cell morphology (Figure 8, A-B). TEM images confirmed that urinary and endothelial-derived EVs have kept their integrity and expected morphology during isolation process. In the result, we obtained pure EVs samples with heterogenous size distribution ranging between $50 - 300\text{ nm}$ for TEM images of EVs isolated from normoglycemic and hyperglycemic *in vitro* conditions (Figure 8, C-D) and ranging between $30 - 200\text{ nm}$ for UEVs isolated from urine of control and urine of diabetic patients (Figure 8, E-F). Both normoglycemic endothelial-derived EVs and control UVs show higher electron density in compare to hyperglycemic or diabetic conditions (Figure 8 C-F).

4. Discussion

In the present study, Raman spectroscopy has been used to detect a specific spectral signature of EVs isolated from urine of T2DM patients and healthy donors. Additionally, Raman spectra of endothelium-derived EVs isolated from normoglycemic and hyperglycemic cell culture media were analyzed.

Urine contains a huge number of metabolites which are listed in The Urine Metabolome Database [38]. Because EVs have the ability to transfer different molecules then those present naturally within body fluids, they may serve as biomarkers of pathological changes in the human body [39]. So far it has been demonstrated that molecular changes in EVs caused by diseases can be distinguished and quantified by Raman spectroscopy method [40]. This non-destructive light scattering technique provides molecular fingerprint of the sample during a real-time measurement.

Average Raman spectra obtained for UEVs from diabetic and control urine samples showed differences for specific bands in the fingerprint region. The biggest difference in the relative intensity was observed for Amide I band (1665 cm^{-1}) which is characteristic for protein secondary structures. CA confirmed that Raman spectroscopy can be used to differentiate EVs from urine of T2DM patients and healthy subjects. In turn, detailed PLS analysis indicated the most distinct difference for proteins, lipids and nucleic acids bands between these study groups.

The control and CD samples showed much higher relative intensities of protein bands in comparison with UD ones, what suggests lower protein content in the UEVs of patients with unsatisfactory glycemic control. Similarly, TEM images of control UEVs show higher electron density in compare to diabetic UEVs. In fact, in the end-stage of diabetic renal damage, the protein concentration in urine is very high because of albuminuria [41]. The

hypothesis would be that UD patients have different protein profile in UEVs. These data are in line with our former observations that protein diversity in UEVs is in opposite to albumin concentration in urine [8]. Moreover, Yu MC et al. observed similar relationship between urine samples from normal and nephrotoxic nephritis treated rats using ATR-FTIR spectroscopy [42].

On the other hand, integral intensity of phenylalanine band is higher for UD samples. Similar patterns have been observed for urine albumin concentration. Such strong positive correlation between aromatic amino acids levels including phenylalanine in plasma and the risk of T2DM development has been previously demonstrated for a cohort of normoglycemic individuals [43]. This data suggests that at least some of the aromatic amino acids are transferred by UEVs as waste of impaired metabolic processes predisposing to diabetic complications development.

Furthermore, we observed higher intensity in the spectra range characteristic for lipids ($1420-1470\text{ cm}^{-1}$) in UD samples, but lower content of cholesterol and its derivatives. Changed levels of lipids in UEVs from UD patients can be associated with dyslipidemia which very often occurs in T2DM [44]. This lipid abnormality is characterized by increased triacylglycerols (TG) and reduced high-density lipoprotein cholesterol (HDL-C) levels in patients with cardiovascular risk [45, 46]. Lipids lowering therapy is recommended as a standard treatment in T2DM, thus statins (lipid lowering drugs) are the most commonly used pharmaceuticals to reduce low-density lipoprotein cholesterol (LDL-C) [47].

Additionally, we observed higher intensity of nucleic acids signal in UEVs from CD samples compared to control and UD groups. It has been previously shown that cell-free plasma and urine DNA is elevated in different pathological states e.g. prostate and bladder cancer or organ transplantations [48]. This suggests that UEVs may be involved in the clearance of

circulating DNA, hence they can be considered as potential carriers of free DNA for molecular diagnostics.

Integral intensities for selected bands corresponded well with results obtained by PLS analysis. We found higher integral intensity of 840-865 cm^{-1} band which may come from 3-hydroxybutyric acid (HA). HA is a main component of ketone bodies present in blood and urine of patients with unsatisfactory glycemic control [36]. The presence of HA in UEVs confirms that EVs are a waste fraction to transport or remove metabolic components from diseases cells. Such mechanism has been previously proposed for microvesicles shed from cancer cells [49].

Our analysis showed, that average Raman spectra of UEVs correlate well with biochemical parameters such as: serum glucose and creatinine concentration in study samples. It confirms that Raman spectroscopy is a powerful tool in UEVs studies for fast differentiation between healthy and diabetic patients. We cannot exclude that epidemiologic factors as age, BMI or gender may have importance in the UEV number or molecular signature. However, in our previous study we did not observe any significant correlations between age and UEVs density both in healthy control or diabetic patients (supplementary data) [8]. In the current study, the control group did not differ from CD or UD and with respect to age ($p=0.116$ and $p=0.203$, respectively).

Within endothelium-derived EVs, slight differences in Raman intensities of some bands have been observed. Our PLS model obtained for EVs isolated from cell culture media was similar to the PLS model for UEVs from diabetic and control samples. This means that cell culture *in vitro* model reflects adequately physiological conditions for CD and UD diabetes. Furthermore, regression coefficient β plots for diabetic patients and cell cultures (Figure 2, C and Figure 6, C) show great similarity between UD and HG short hyperglycemic conditions.

However, some differences were observed here, such as presence of carbohydrates in endothelium-derived EVs and HA in UEVs.

PLS analysis indicated specific bands derived from saccharides, proteins, proteins α -helix conformation, lipids and nucleic acids which allow to separate studied groups. Based on PLS analysis, the most characteristic molecular signature was observed for HG short hyperglycemic cell culture medium. There were significantly higher levels of saccharides and lipids in HG short samples in comparison with NG and HG long samples.

Based on our study, we may assume that Raman spectroscopy distinguishes CD and UD diabetic patients as well as between diabetics and healthy subjects. Results obtained for endothelium-derived EVs showed also the potential of Raman spectroscopy technique to be used to differentiate cells cultured in different glycemic conditions. Our investigation confirmed, that Raman spectroscopy is a powerful tool for searching abnormalities in UEVs derived from pathologically altered tissues, what can be very useful for diagnosis of diabetic complications at an early stage.

Acknowledgements:

The authors would like to thank Aleksandra Tokarz for clinical database of patients and Olga Woźnicka from Institute of Zoology and Biomedical Research of the Jagiellonian University for providing TEM images. Many thanks for Centre for Technology Transfer CITTRU of the Jagiellonian University for support in patent application no. 423 634.

References

1. Combes, A, Simon AC, Grau GE, Arnoux D, Camoin L, Sabatier FF, et al. In vitro generation of endothelial microparticles and possible prothrombotic activity in patients with lupus anticoagulant. *J Clin Invest* 1999;**104**:93-102
2. Gross JC, Chaudhary V, Bartscherer K, Boutros M. Active Wnt proteins are secreted on exosomes. *Nat Cell Biol* 2012;**14**:1036-45.
3. Pisetsky DS, Ullal AJ, Gauley J, Ning TC. Microparticles as mediators and biomarkers of rheumatic disease. *Rheumatology (Oxford)* 2012;**51**:1737–46.
4. Lacroix R, Sabatier F, Mialhe A, Basire A, Pannell R, Borghi H, et al. Activation of plasminogen into plasmin at the surface of endothelial microparticles: a mechanism that modulates angiogenic properties of endothelial progenitor cells in vitro. *Blood* 2007;**110**:2432-9.
5. Barreiro K, Holthofer H. Urinary extracellular vesicles. A promising shortcut to novel biomarker discoveries. *Cell Tissue Res* 2017;**369**:217-27.
6. Salih M, Zietse R, Hoorn EJ. Urinary extracellular vesicles and the kidney: biomarkers and beyond. *Am J Physiol Renal Physiol* 2014;**306**:1251-9.
7. Sun H, Yao W, Tang Y, Zhuang W, Wu D, Huang S, et al. Urinary exosomes as a novel biomarker for evaluation of α -lipoic acid's protective effect in early diabetic nephropathy. *J Clin Lab Anal* 2017;**31**, doi: 10.1002/jcla.22129.
8. Kamińska A, Platt M, Kasprzyk J, Kuśnierz-Cabala B, Gala-Błądzińska A, Woźnicka O, et al. Urinary Extracellular Vesicles: Potential Biomarkers of Renal Function in Diabetic Patients. *J Diabetes Res* 2016;**2016**:5741518.
9. Zhou H, Pisitkun T, Aponte A, Yuen PS, Hoffert JD, Yasuda H, et al. Exosomal Fetuin-A identified by proteomics: a novel urinary biomarker for detecting acute kidney injury. *Kidney Int* 2006;**70**:1847-57.

10. Sekuła M, Janawa G, Stankiewicz E, Stępień E. Endothelial microparticle formation in moderate concentrations of homocysteine and methionine in vitro. *Cell Mol Biol Lett* 2011;**16**:69-78.
11. Sabatier F., Darmonu P., Hugel B., Combes V., Sanmarco M., Velut J.-G. et.al.: Type 1 and type 2 diabetic patients display different patterns of cellular microparticles. *Diabetes* 2002;**51**:2840-2845.
12. Hromada C, Muhleder S, Grillari J, Redl H, Holnthoner W. Endothelial Extracellular Vesicles-Promises and Challenges. *Front Physiol* 2017;**8**:275.
13. Sunkara V, Woo HK, Cho YK. Emerging techniques in the isolation and characterization of extracellular vesicles and their roles in cancer diagnostics and prognostics. *Analyst* 2016;**141**(2):371-81.
14. Rupert DLM, Claudio V, Lässer C, Bally M. Methods for the physical characterization and quantification of extracellular vesicles in biological samples. *Biochim Biophys Acta* 2017; **1861**(1):3164-3179.
15. Szatanek R, Baj-Krzyworzeka M, Zimoch J, Lekka M, Siedlar M, Baran J. Methods of choice for extracellular vesicles (EVs) characterization. *Int J Mol* 2017;**18**(6):1153.
16. Puppels GJ, Demul FFM, Otto C, Greve J, Robert-Nicoud M, Arndt-Jovin DJ, et al. Studying single living cells and chromosomes by confocal Raman microspectroscopy. *Nature* 1990;**347**(6290),301–3.
17. Tatischeff I, Larquet E, Falcón-Pérez JM, Turpin PY, Kruglik SG. Fast characterisation of cell-derived extracellular vesicles by nanoparticles tracking analysis, cryo-electron microscopy, and Raman tweezers microspectroscopy. *J Extracell Vesicles* 2012;**1**:19179.

18. Smith ZJ, Lee C, Rojalin T, Carney RP, Hazari S, Knudson A, et al. Single exosome study reveals subpopulations distributed among cell lines with variability related to membrane content. *J Extracell Vesicles* 2015;**4**:28533.
19. Tu Q, Chang C. Diagnostic application of Raman Spectroscopy. *Nanomedicine* 2012;**8**:545-58.
20. Virkler K, Lednev IK. Raman spectroscopic signature of blood and its potential application to forensic body fluid identification. *Anal Bioanal Chem* 2010;**396**:525-34.
21. Muro CK, Lednev IK. Identification of individual red blood cells by Raman microspectroscopy for forensic purposes: in search of a limit of detection. *Anal Bioanal Chem* 2017;**409**(1):287-93.
22. Barman I, Dingari NC, Kang JW, Horowitz GL, Ramachandra RD, Feld MS. Raman Spectroscopy-Based Sensitive and Specific Detection of Glycated Hemoglobin. *Anal Chem* 2012;**84**(5):2474-82.
23. Dingari NC, Horowitz GL, Kang JW, Dasari RR, Barman I. Raman Spectroscopy Provides a Powerful Diagnostic Tool for Accurate Determination of Albumin Glycation. *PLoS ONE* 2012; **7**:e32406.
24. Lin J, Lin J, Huang Z, Lu P, Wang J, Wang X, et al. Raman spectroscopy of human hemoglobin for diabetes detection. *Innov Opt Health Sci* 2014;**7**:1350051.
25. Brindha E, Rajasekaran R, Aruna P, Koteeswaran D, Ganesan S. High wavenumber Raman spectroscopy in the characterization of urinary metabolites of normal subjects, oral premalignant and malignant patients. *Spectrochim Acta, Part A* 2017;**171**:52-9.
26. 2016 Guidelines on the management of diabetic patients. A position of diabetes Poland. *Diabetologia Kliniczna* 2016; 5 (supl. A): A1-A73.

27. Musante L, Tataruch D, Gu D, Benito-Martin A, Calzaferri G, Sinead A, et al. A Simplified Method to Recover Urinary Vesicles for Clinical Applications, and Sample Banking. *Sci Rep* 2014;**4**:7532.
28. Coumans FA, van der Pol E, Böing AN, Hajji N, Sturk G, van Leeuwen TG, Nieuwland R. Reproducible extracellular vesicle size and concentration determination with tunable resistive pulse sensing. *J Extracell Vesicles* 2014;**3**:25922.
29. Blundell ELCJ, Mayne LJ, Billinge ER, Platt M. Emergence of tunable resistive pulse sensing as a biosensor. *Anal Methods* 2015;**7**:7055-66.
30. Blundell ELCJ, Vogel R, Platt M. Particle-by-Particle Charge Analysis of DNA-Modified Nanoparticles Using Tunable Resistive Pulse Sensing. *Langmuir* 2016;**32**:1082-90.
31. Notingher I. Raman Spectroscopy Cell-based Biosensors. *Sensors* 2007;**7**(8):1343-58.
32. Matthaus C, Bird B, Miljkovic M, Chernenko T, Romeo M, Diem M. Chapter 10: Infrared and Raman microscopy in cell biology. *Methods Cell Biol* 2008;**89**:275-308.
33. Rygula A, Majzner K, Marzec KM, Kaczor A, Pilarczyk M, Baranska M. Raman spectroscopy of proteins: a review. *J Raman Spectrosc* 2013;**44**(8):1061-76.
34. Czamara K, Majzner K, Pacia MZ, Kochan K, Kaczor A, Baranska M. Raman spectroscopy of lipids: a review. *J Raman Spectrosc* 2015;**46**:4-20.
35. De Gelder J, Willemsse-Erix D, Scholtes MJ, Sanchez JI, Maquelin K, Vandenabeele P, et al. Monitoring poly(3-hydroxybutyrate) production in *Cupriavidus necator* DSM 428 (H16) with raman spectroscopy. *Anal Chem* 2008;**80**(6):2155-60.
36. Sheikh-Ali M, Karon BS, Basu A, Kudva YC, Muller LA, Xu J, et al. Can serum beta-hydroxybutyrate be used to diagnose diabetic ketoacidosis. *Diabetes Care* 2008;**31**(4):643-47.

37. Wiercigroch E, Szafraniec E, Czamara K, Pacia MZ, Majzner K, Kochan K, et al. Raman and infrared spectroscopy of carbohydrates: A review. *Spectrochim Acta Part A* 2017;**185**:317–35.
38. Bouatra S, Aziat F, Mandal R, Guo AC, Wilson MR, Craig K, et al. The Human Urine Metabolome. *PLoS ONE* 2013;**8**(9):e73076.
39. Gamez-Valero A, Lozano I, Bancu I, Lauzurica-Valdemoros R, Borrás FE. Urinary extracellular vesicles as source of biomarkers in kidney diseases. *Front Immunol* 2015;**6**:6.
40. Krafft C, Wilhelm K, Eremin A, Nestel S, von Bubnoff N, Schultze-Seemann W, et al. A specific spectral signature of serum and plasma-derived extracellular vesicles for cancer screening. *Nanomedicine* 2017;**13**(3):835-41.
41. Carrero JJ, Grams ME, Sang Y, Ärnlöv J, Gasparini A, Matsushita K, et al. Albuminuria changes are associated with subsequent risk of end-stage renal disease and mortality. *Kidney Int* 2017;**91**:244-251.
42. Yu MC, Rich P, Foreman L, Smith J, Yu MS, Tanna A, et al. Label Free Detection of Sensitive Mid-Infrared Biomarkers of Glomerulonephritis in Urine Using Fourier Transform Infrared Spectroscopy. *Sci Rep* 2017;**7**:4601 doi: 10.1038/s41598-017-04774-7.
43. Wang TJ, Larson MG, Vasan RS, Cheng S, Rhee EP, McCabe E, et al. Metabolite profiles and the risk of developing diabetes. *Nat Med* 2011;**17**:448-53.
44. Rivelles AA, Vaccaro O, Patti L. The pathophysiology of lipid metabolism and diabetes. *Int J Clin Pract* 2004;**58**:32-35.
45. Vergès B. Pathophysiology of diabetic dyslipidemia: where are we? *Diabetologia* 2015;**58**:886-899.

46. Parhofer KG. Interaction between glucose and lipid metabolism: more than diabetic dyslipidemia. *Diabetes Metab J* 2015;**39**:353-362.
47. Subedi BH, Tota-Maharaj R, Silverman MG, Minder CM, Martin SS, Ashen MD, et al. The role of statins in diabetes treatment. *Diabetes Spectr* 2013;**26**:156-164.
48. Chan AKC, Chiu RWK, Lo YMD. Cell free nucleic acids in plasma, serum and urine: a new tool in molecular diagnosis. *Ann Clin Biochem* 2003;**40**:122-130.
49. Shedden K, Xie XT, Chandaroy P, Chang YT, Rosania GR. Expulsion of small molecules in vesicles shed by cancer cells: association with gene expression and chemosensitivity profiles. *Cancer Res* 2003;**63**:4331-4337.

ACCEPTED MANUSCRIPT

Figure legends

Figure 1. The average Raman spectra of UEVs isolated from C, CD and UD study groups (A), dendrogram obtained from CA analysis (B).

Figure 2. Comparison of predicted and assigned variables for C, CD and UD study groups obtained from PLS analysis (CD-C-UD model – A, CD-UD-C model - D), cumulative variance percentage as a function of the latent variables (CD-C-UD model – B, CD-UD-C model - E), regression coefficients β calculated from the models (CD-C-UD model – C, CD-UD-C model - F).

Figure 3. Regression coefficients β calculated from the models for C-CD samples pair (A), C-UD samples pair (B), and CD-UD samples pair (C).

Figure 4. Comparison of predicted and measured clinical parameters (A, C, E) as well as regression coefficients β (B, D, F) calculated from PLS models for correlations between Raman spectra of C, UD, CD samples and: serum glucose (A-B), urine albumin (C-D), urine creatinine (E-F).

Figure 5. The average Raman spectra of EVs isolated from NG, HG long and HG short study groups (A), dendrogram obtained from CA analysis (B).

Figure 6. Comparison of predicted and assigned variables for NG, HG long and HG short study groups obtained from PLS analysis (A), cumulative variance percentage as a function of the latent variables (B), regression coefficient β calculated from the model (C).

Figure 7. Regression coefficients β calculated from the models for NG-HG short samples pair (A), HG long-HG short samples pair (B), and NG-HG long samples pair (C).

Figure 8. Representative optical microscopy images of HUVEC cell culture in normoglycemic (A) and hyperglycemic (B) conditions. Transmission electron micro images of EVs isolated from normoglycemic (C) and hyperglycemic endothelial conditioned medium (D) – endothelial-derived EVs; UVS from urine of a healthy subject (E) and a diabetic patient (F). TEM images visualized the heterogenous population of EVs in diameter 30 – 300 nm.

ACCEPTED MANUSCRIPT

Table 1. Clinical characteristics, blood, and urine biochemistry of study groups: C, CD, and UD group

	C	CD	UD	p-value
Gender Male/Female (n)	5/5	13/6	18/8	-----
Age (years)	51 (7)	62 (16)	61 (13)	0.099
HbA1c (mmol/mol)	-----	44.0* (42.0-48.0)	68.0* (61.8-73.3)	<0.0001
HbA1c (%)	-----	6.2* (6.0-6.5)	8.4* (7.8-8.8)	<0.0001
Serum glucose (mmol/L)	5.2 (5.0-5.5)	6.8*† (5.9-7.6)	8.8*† (7.2-11.4)	<0.0001
Urine albumin (mg/L)	6.2 (4.2-13.4)	6.0* (1.4-10.1)	29.9*† (12.2-243.5)	0.0002
Urine creatinine (mmol/L)	12.2 (9.3-16.0)	5.4† (4.2-10.1)	6.3† (4.8-9.6)	0.01
Serum creatinine (μmol/L)	68.5 (60.1-85.1)	73.4 (61.9-86.6)	76.5 (60.6-103.6)	0.546
eGFR (mL/min/1.73 m ²)	83.9 (76.1-100.5)	89.2 (68.0-102.9)	86.1 (63.6-99.9)	0.921
EVs concentration (number/mL)	1.11E11 (3.6E10-2.7E10)	8.7E10 (5.2E10-2.3E11)	7.4E10 (3.0E10-1.7E22)	0.499
EVs median diameter (nm)	121 (119-123)	135† (127-143)	128† (126-134)	0.0003

Differences between subgroups were tested with the t-Student or Mann-Whitney U tests.

*statistically significant difference between CD and UD group (p-value detailed in the text)

† statistically significant difference with comparison to the control group (p-value detailed in the text)

p-value tested using the Kruskal-Wallis or one-way ANOVA tests. Bold means statistically significant difference between all study groups at $\alpha < 0.05$ level.

ACCEPTED MANUSCRIPT

Urine has shown to be a particularly rich reservoir of extracellular vesicles (EVs) which are potential biomarkers of diabetes and its renal complications. EVs were isolated by Hydrostatic Filtration Dialysis and ultracentrifugation method. Raman spectroscopy was applied to the measurement of spectral signatures of vesicles. Partial Least Squares regression and Cluster Analysis were used for detailed analysis of all chemical differences between study samples. Raman spectroscopy allowed to distinguish diabetic patients (with good and unsatisfactory glycemic control) and healthy subjects. Additionally we showed the potential of Raman spectroscopy technique to be used to differentiate cells cultured in different glycemic conditions.

ACCEPTED MANUSCRIPT

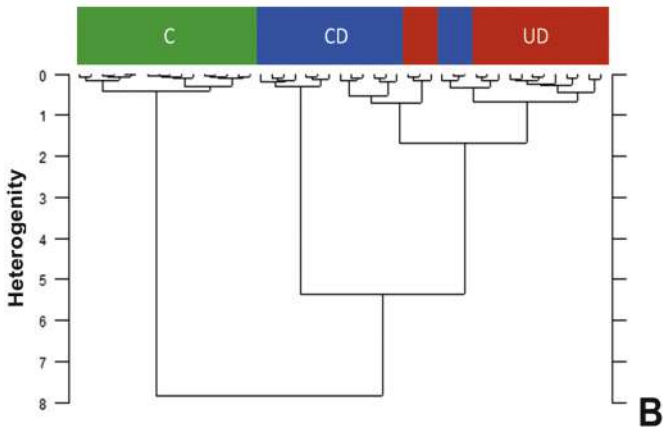
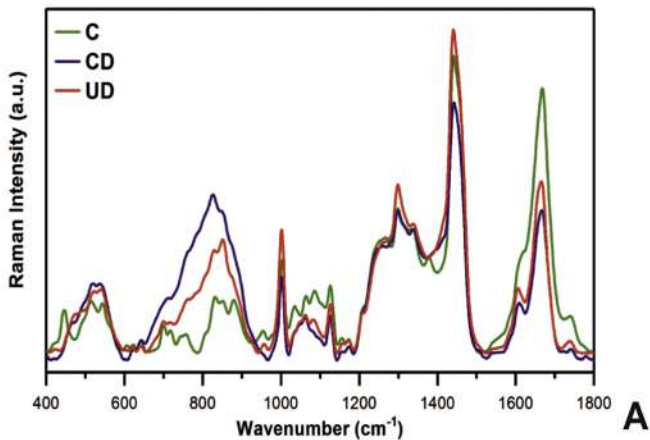


Figure 1

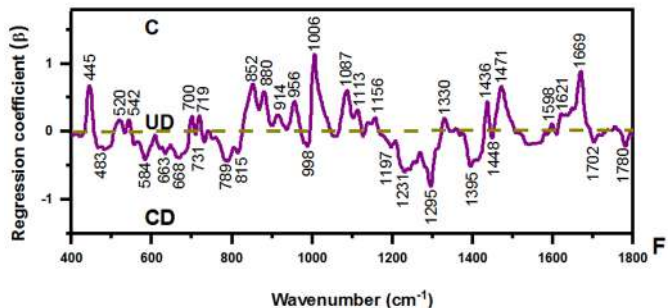
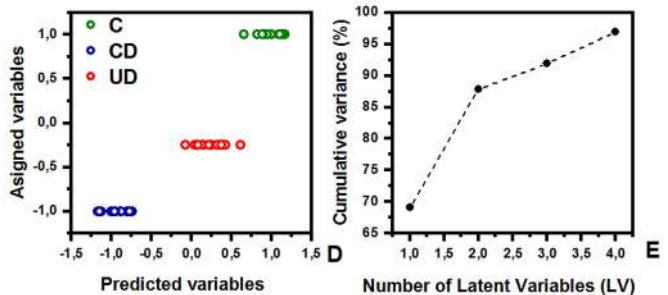
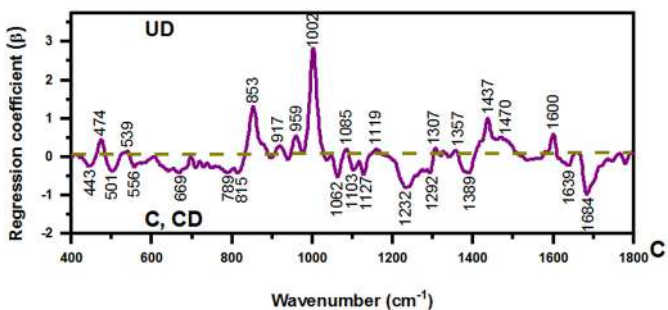
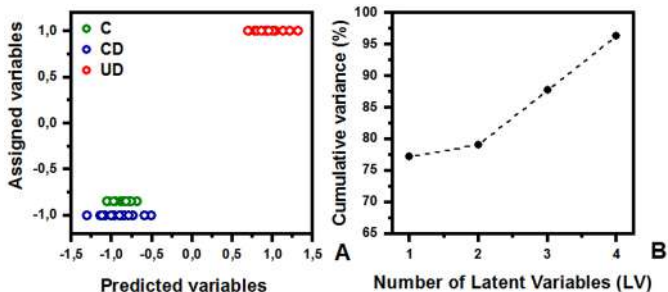


Figure 2

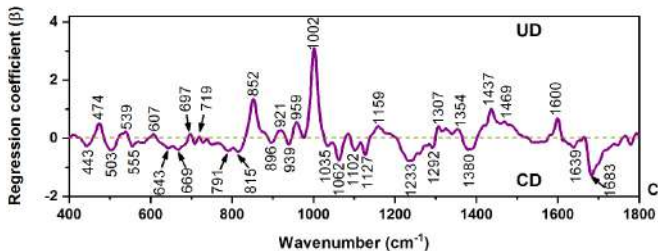
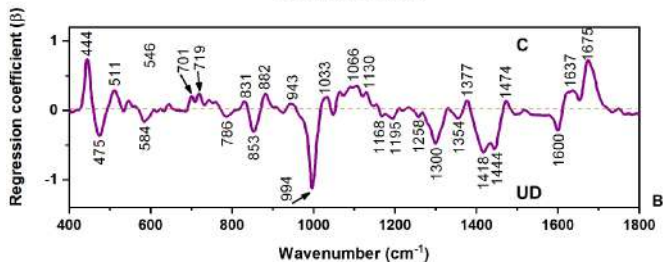
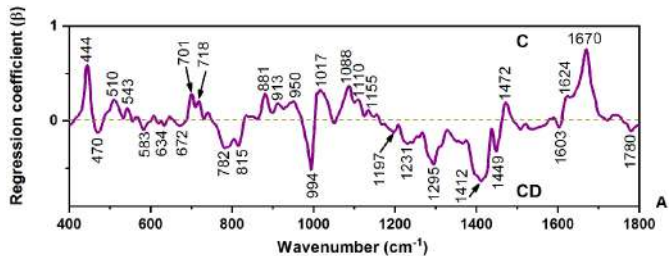


Figure 3

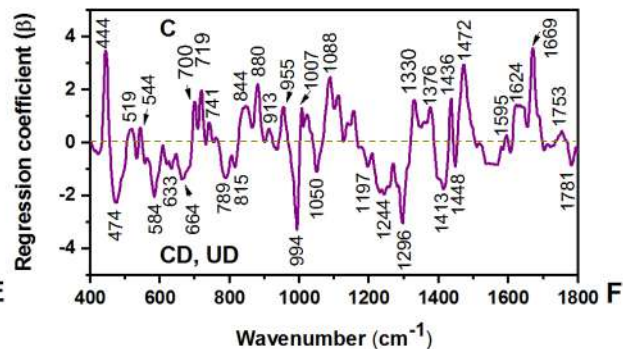
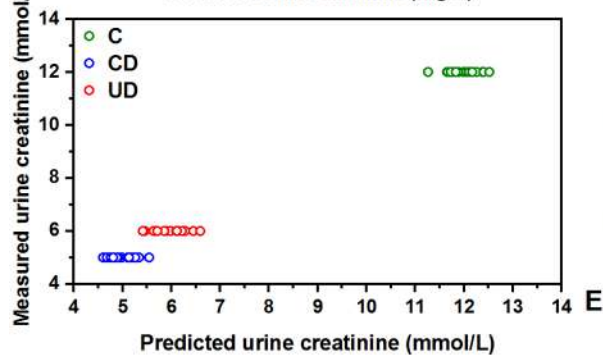
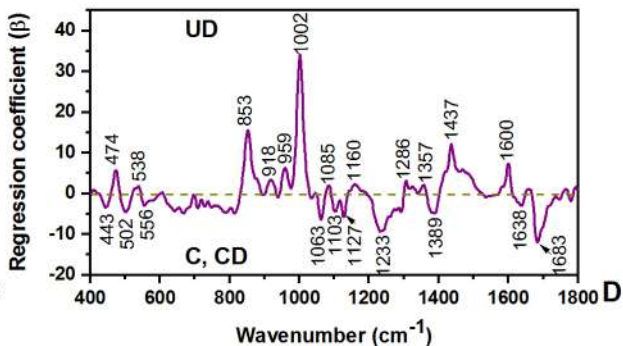
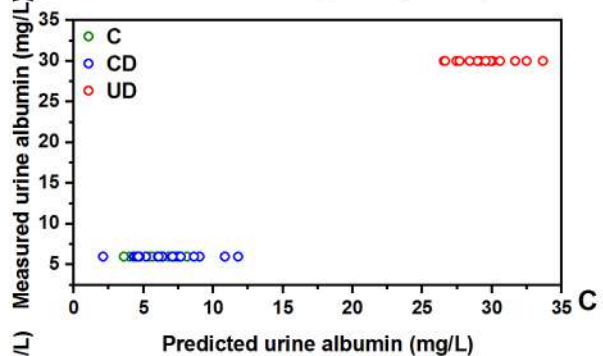
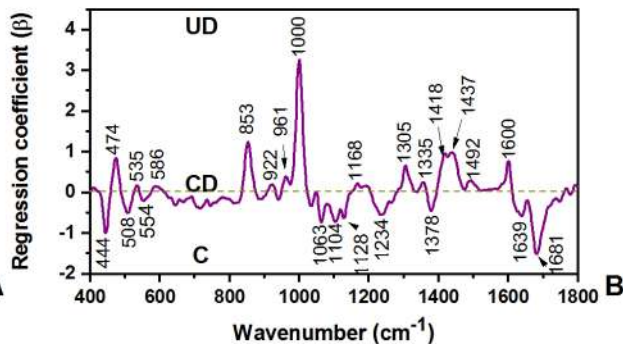
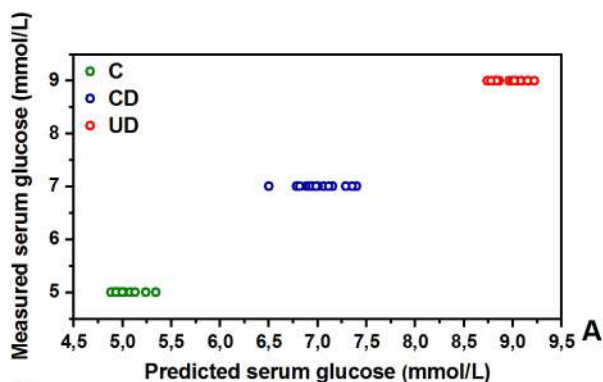


Figure 4

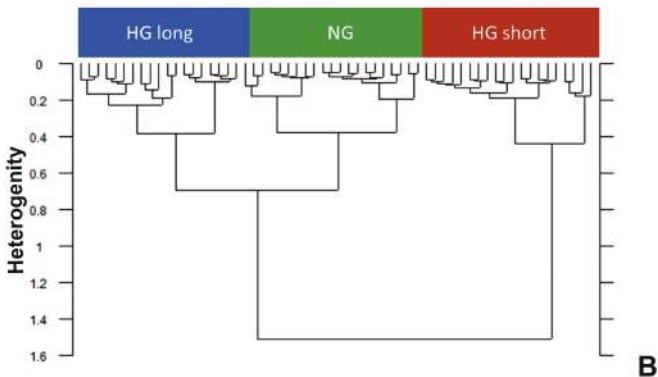
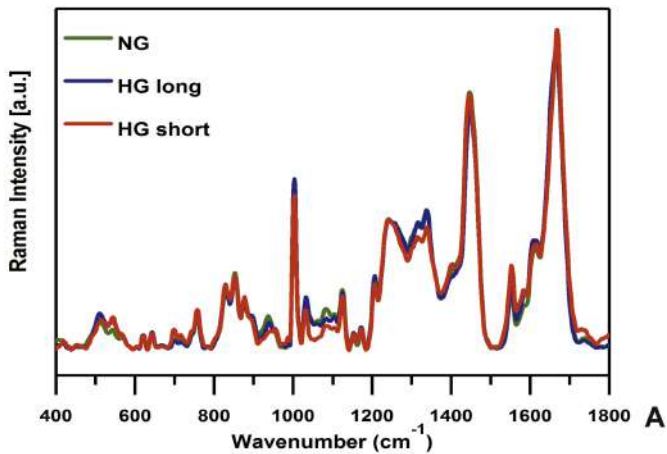


Figure 5

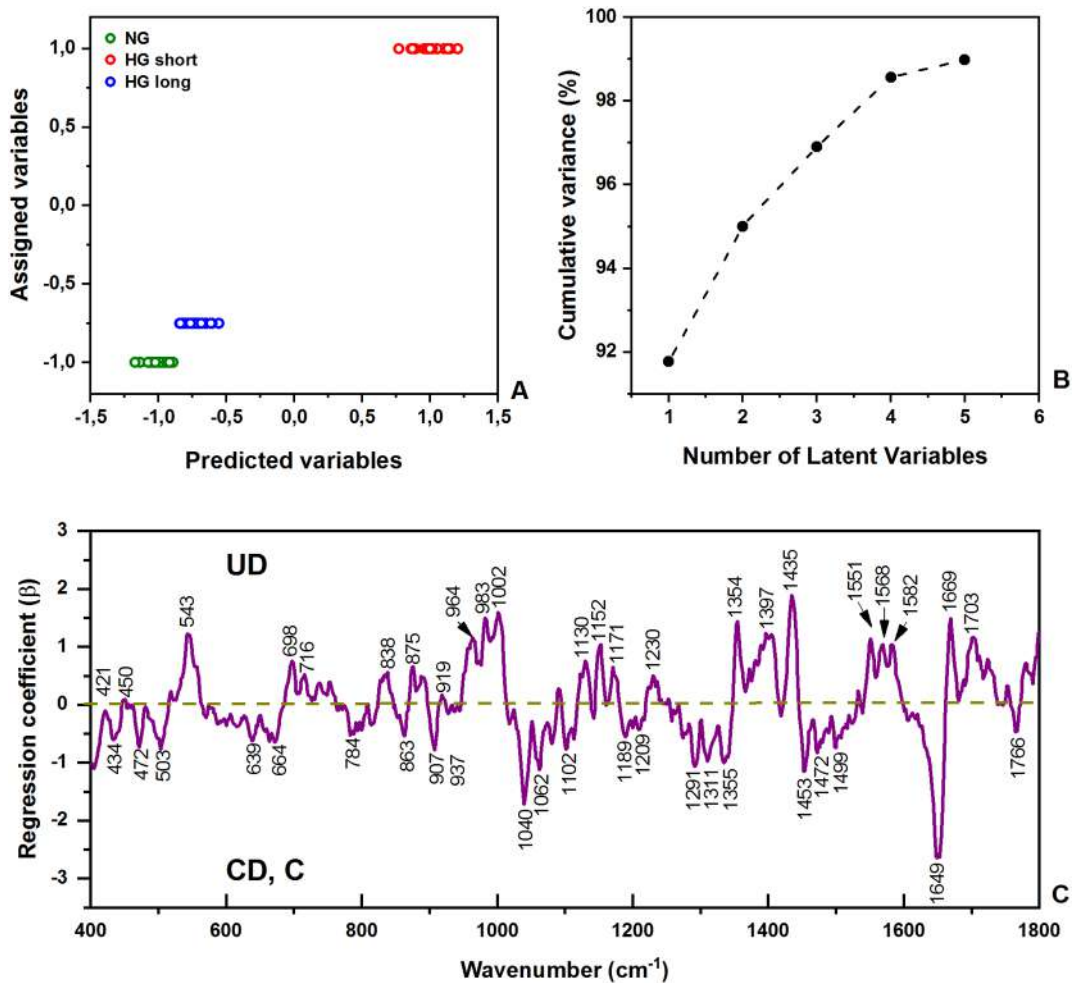


Figure 6

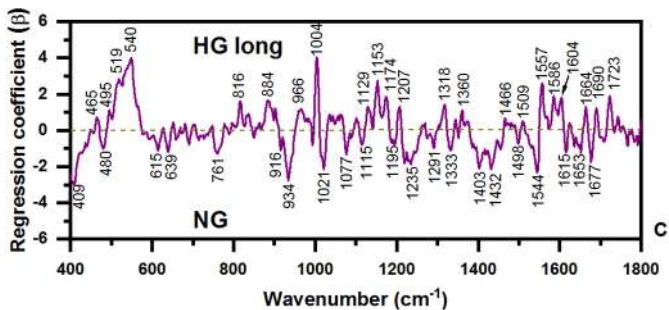
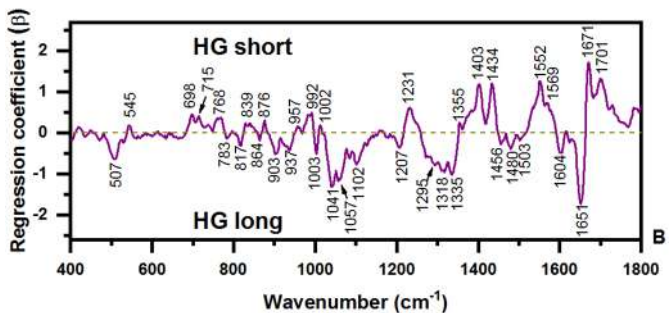
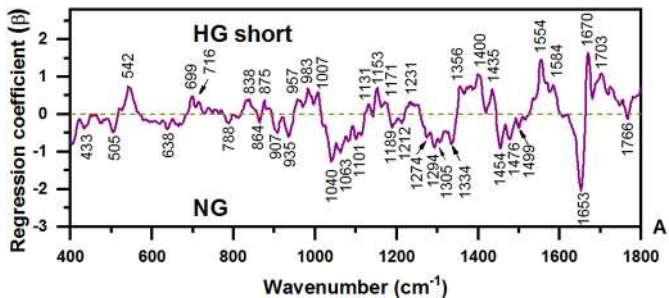


Figure 7

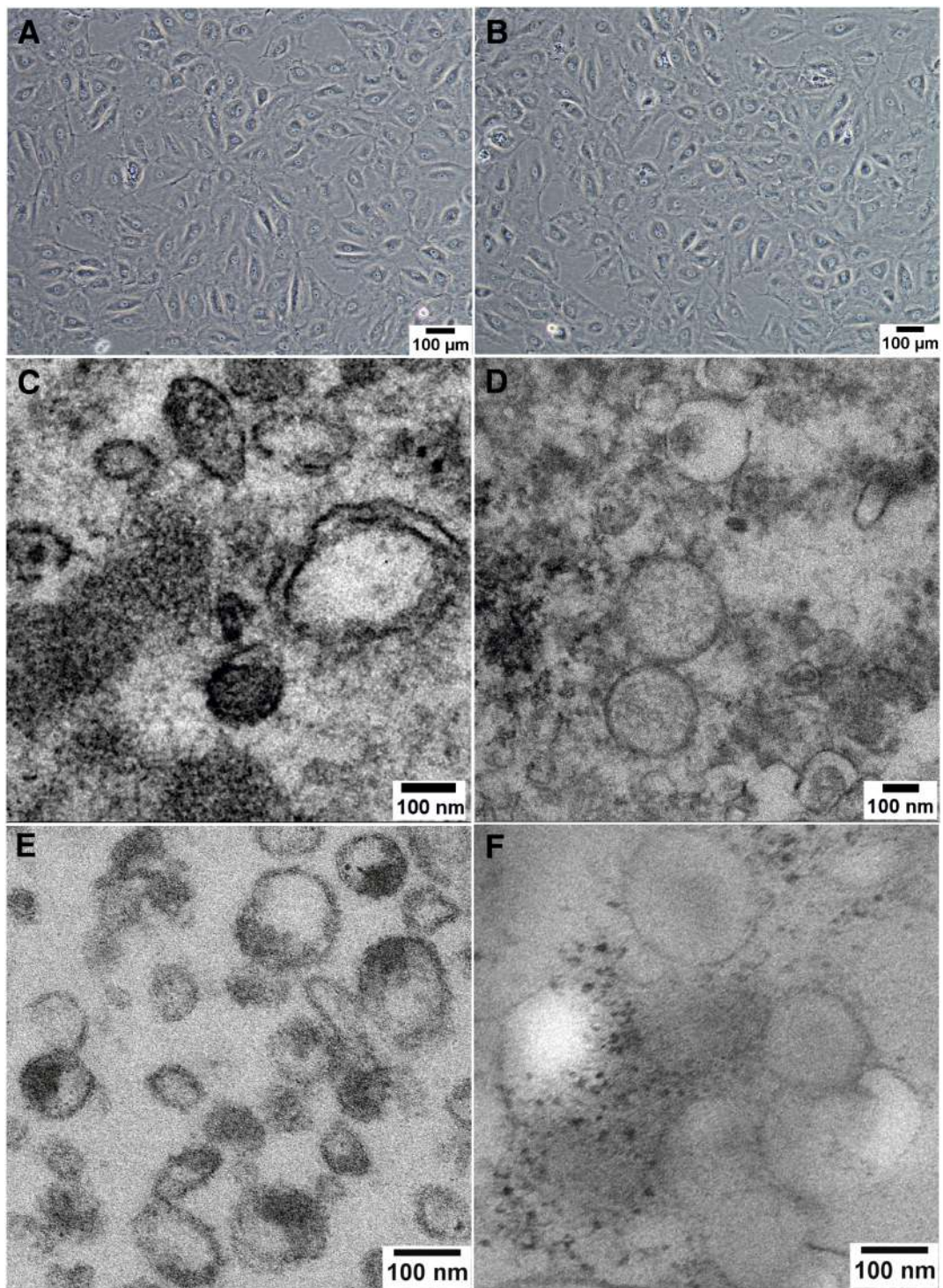


Figure 8